

Targeting the D Series Resolvin Receptor System for the Treatment of Osteoarthritis Pain

Junting Huang, James J. Burston, Li Li, Sadaf Ashraf, Paul I. Mapp,
Andrew J. Bennett, Srinivasarao Ravipati, Petros Pousinis, David A. Barrett,
Brigitte E. Scammell, and Victoria Chapman

Objective. Pain is a major symptom of osteoarthritis (OA); currently available analgesics either do not provide adequate pain relief or are associated with serious side effects. The aim of this study was to investigate the therapeutic potential of targeting the resolvin receptor system to modify OA pain and pathology.

Methods. Gene expression of 2 resolvin receptors (ALX and ChemR23) was quantified in synovium and medial tibial plateau specimens obtained from patients with OA at the time of joint replacement surgery. Two models of OA joint pain were used for the mechanistic studies. Gene expression in the joint and central nervous system was quantified. The effects of exogenous administration of the D series resolvin precursor 17(R)-hydroxy-docosahexaenoic acid (17[R]-HDoHE) on pain behavior, joint pathology, spinal microglia, and astroglia were quantified. Plasma levels of relevant lipids, resolvin D2, 17(R)-HDoHE, and arachidonic acid, were determined in rats, using liquid chromatography tandem mass spectrometry.

Results. There was a positive correlation between resolvin receptor and interleukin-6 (IL-6) expression in human OA synovial and medial tibial plateau tissue. In rats, synovial expression of ALX was positively correlated with expression of IL-1 β , tumor necrosis factor, and cyclooxygenase 2. Treatment with 17(R)-HDoHE reversed

established pain behavior (but not joint pathology) in 2 models of OA pain. This was associated with a significant elevation in the plasma levels of resolvin D2 and a significant reduction in astroglia in the spinal cord in the monosodium iodoacetate-induced OA rat model.

Conclusion. Our preclinical data demonstrate the robust analgesic effects of activation of the D series resolvin pathways in 2 different animal models of OA. Our data support a predominant central mechanism of action in clinically relevant models of OA pain.

Osteoarthritis (OA) is a highly prevalent degenerative joint disorder characterized by loss of cartilage, subchondral bone remodeling, and synovial inflammation (1,2). Pain is the predominant symptom of OA, which limits movement and causes disability (3). OA pain is significantly associated with synovial inflammation and changes in the subchondral bone (4), and evidence of central sensitization and the spread of pain has been reported (5). Existing drugs are poorly effective and/or are associated with adverse side effects. Most often, total joint replacement is the only successful therapeutic treatment (6).

Resolvins are endogenous specialized pro-resolution lipid mediators derived from docosahexaenoic acid (DHA [D series resolvins]) and eicosapentaenoic acid (EPA [E series resolvins]), which exhibit potent antiinflammatory and pro-resolution properties (7,8). Four resolvin receptors have been identified: ALX (also known as *N*-formyl peptide receptor 2), G protein-coupled receptor 32 (GPR32) (9–11), chemokine-like receptor 1 (ChemR23) (12), and leukotriene B₄ receptor (BLT-1) (13). Resolvin D1 (RvD1) binds to and activates both ALX and GPR32 in human tissue, while in murine tissue the actions of RvD1 are mediated by ALX (14). ChemR23 and BLT-1 are the receptors through which RvE1 and RvE2 act (14).

In the context of their therapeutic potential for pain management, RvE1 and RvD1 (administered

Supported by Arthritis Research UK (grant 18769).

Junting Huang, PhD (current address: University of Calgary, Calgary, Alberta, Canada), James J. Burston, PhD, Li Li, PhD, Sadaf Ashraf, PhD, Paul I. Mapp, PhD, Andrew J. Bennett, PhD, Srinivasarao Ravipati, PhD, Petros Pousinis, PhD, David A. Barrett, PhD, Brigitte E. Scammell, DM, FRCS(Orth), Victoria Chapman, PhD: University of Nottingham, Nottingham, UK.

Address correspondence to James J. Burston, PhD, Cardiff University School of Medicine, College of Biomedical and Life Sciences, Tenovus Building, Cardiff CF14 4NX, UK. E-mail: BurstonJ3@cardiff.ac.uk; or to Victoria Chapman, PhD, Arthritis Research UK Pain Centre and School of Life Sciences, The University of Nottingham, Queen's Medical Centre, Nottingham NG7 2UH, UK. E-mail: victoria.chapman@nottingham.ac.uk.

Submitted for publication March 8, 2016; accepted in revised form November 10, 2016.

exogenously) attenuate pain behavior in models of acute inflammatory pain (15,16) and a model of chronic adjuvant-induced arthritis (17). RvD1 inhibits the activity of some temperature-sensitive transient receptor potential (TRP) ion channels expressed by the primary afferent sensory fibers TRP ankyrin 1 (TRPA-1) (18) and TRP vanilloid channel 3 (TRPV-3) (19), but not TRPV-1. Due to the rapid degradation of resolvins, local (intraplantar or intrathecal) routes of administration have been studied. Spinal administration of RvE1 reduced capsaicin- and tumor necrosis factor (TNF)-induced spontaneous pain and hypersensitivity in mice and partially attenuated pain behavior in models of neuropathic pain (20). RvD1 and RvE1 can modulate TRPV-1 and TNF responses in the spinal cord (20–22) and inhibit phosphorylation of *N*-methyl-D-aspartate receptors and cytokine expression in the spinal cord in the setting of chronic pancreatitis-induced pain (23). Thus, both peripheral and spinal mechanisms of action contribute to the inhibitory effects of the resolvins in models of inflammatory and neuropathic pain, with predominant peripheral antiinflammatory mechanisms including inhibition of neutrophil infiltration, edema, and proinflammatory cytokine expression (21).

The therapeutic potential of exogenously administered RvD1 and RvE1 may be limited by instability and short durations of action. Treatment with precursors of the active molecules offers an alternative longer-lasting and beneficial approach (17), as does the development of chemically and metabolically stable analogs such as 17R-hydroxy-19-para-fluorophenoxy-resolvin D1 (24). Inhibitory effects of a precursor of RvD1, 17(R)-hydroxy-docosahexaenoic acid (17[R]-HDoHE), on mechanical hyperalgesia in a model of inflammatory joint pain have been reported and associated with reductions in hind paw levels of TNF and interleukin-1 β (IL-1 β) and spinal cord expression of NF- κ B and cyclooxygenase 2 (COX-2) (17). These data suggest that exogenous augmentation of resolvin precursors has therapeutic potential for the treatment of pain states that are underpinned by peripheral and/or central sensitization mechanisms.

The aim of the current study was to provide new clinical and preclinical evidence for the therapeutic potential of the D series resolvin pathway for the treatment of OA pain. Using 2 different clinically relevant models of OA joint pain, we performed mechanistic studies to interrogate the contribution of peripheral joint versus spinal cord sites of action of this novel class of analgesics.

PATIENTS AND METHODS

Subjects. Research using clinical samples was approved by generic ethics committees for the Nottingham University

Hospitals NHS Trust Biobank (reference no. RSCH 488). Human synovial tissue and bone from the medial tibial plateau were obtained from 15 patients who underwent total knee replacement (TKR) surgery for OA pain. These tissues were selected on the basis of established associations between inflammation, bone remodeling, and pain (1,2). Fresh tissue samples were collected from the surgical team and snap-frozen and stored in a -80°C freezer at the Biobank, City Hospital, University of Nottingham. Fresh synovial tissue specimens ($n = 15$) and medial tibial plateau specimens ($n = 14$) were used to quantify gene expression.

Animals and model induction. Animal experiments were approved by the Nottingham University ethics committee, and all procedures were approved by the UK Home Office in accordance with the Animals (Scientific Procedures) Act 1986 and conform to the guidelines of the International Association for the Study of Pain. Adult male Sprague-Dawley rats ($n = 166$) were used (Charles River). All procedures and testing were performed in a blinded manner. The model of monosodium iodoacetate (MIA)-induced OA pain was generated as previously described (25). The medial meniscal transection (MNX) induction model of OA pain was based on previously described methods (26) (see also Supplementary Methods, available on the *Arthritis & Rheumatology* web site at <http://onlinelibrary.wiley.com/doi/10.1002/art.40001/abstract>).

Pharmacologic interventions and assessment of pain behavior. Weight-bearing asymmetry and hind paw mechanical withdrawal thresholds were determined using a Linton incapacitance tester and von Frey monofilaments (Linton Instrumentation; bending force 1–26g, respectively) as previously described (27) (see Supplementary Methods). An RvD1 precursor, 17(R)-HDoHE, also known as 17(R)-HDHA, was purchased from Cayman Chemical. This precursor gives rise to the production of 17R RvD1 and 17R RvD2, epimers of endogenous RvD1, RvD2, RvD3, and RvD4 (synthesized from 17[S]-HDoHE), and aspirin-triggered epimers (17R forms), when COX-2 is acetylated (14).

The 17(R)-HDoHE (stock solution 100 $\mu\text{g}/\text{ml}$ in ethanol) was diluted in normal sterile saline to provide a concentration of 1 $\text{ng}/\mu\text{l}$. The vehicle solution consisted of 1% ethanol solution in 99% saline. A series of different pharmacologic studies were performed using 300 ng of 17(R)-HDoHE in 300 μl saline administered intraperitoneally. Study 1 determined the effects of a single injection of 17(R)-HDoHE on pain behavior on day 14 after induction of the model. Study 2 determined the effects of repeated administration of 17(R)-HDoHE (300 ng in 300 μl saline, every other day from day 14 until day 28 after induction of the model) on pain behavior in the MIA-induced OA pain model and the MNX induction model of OA pain. Study 3 determined the effects of discontinuous administration of 17(R)-HDoHE (300 ng in 300 μl saline, from day 14 to day 22 after induction of the model) on pain behavior, quantified until day 35 after induction of the model. All of the drug intervention studies were conducted in a blinded manner.

Quantitative real-time polymerase chain reaction. At the end of the behavioral studies, the rats were killed via an overdose of sodium pentobarbital, and fresh-frozen spinal cords and synovial tissue were collected and stored at -80°C . Tissues were homogenized in ice-cold TRI Reagent to extract total RNA from the samples, as previously described (26). Human OA synovial tissue collected at the time of TKR surgery was homogenized in cold TRI Reagent, and RNA was extracted as previously described. Bone from the mid part of the medial tibial plateau

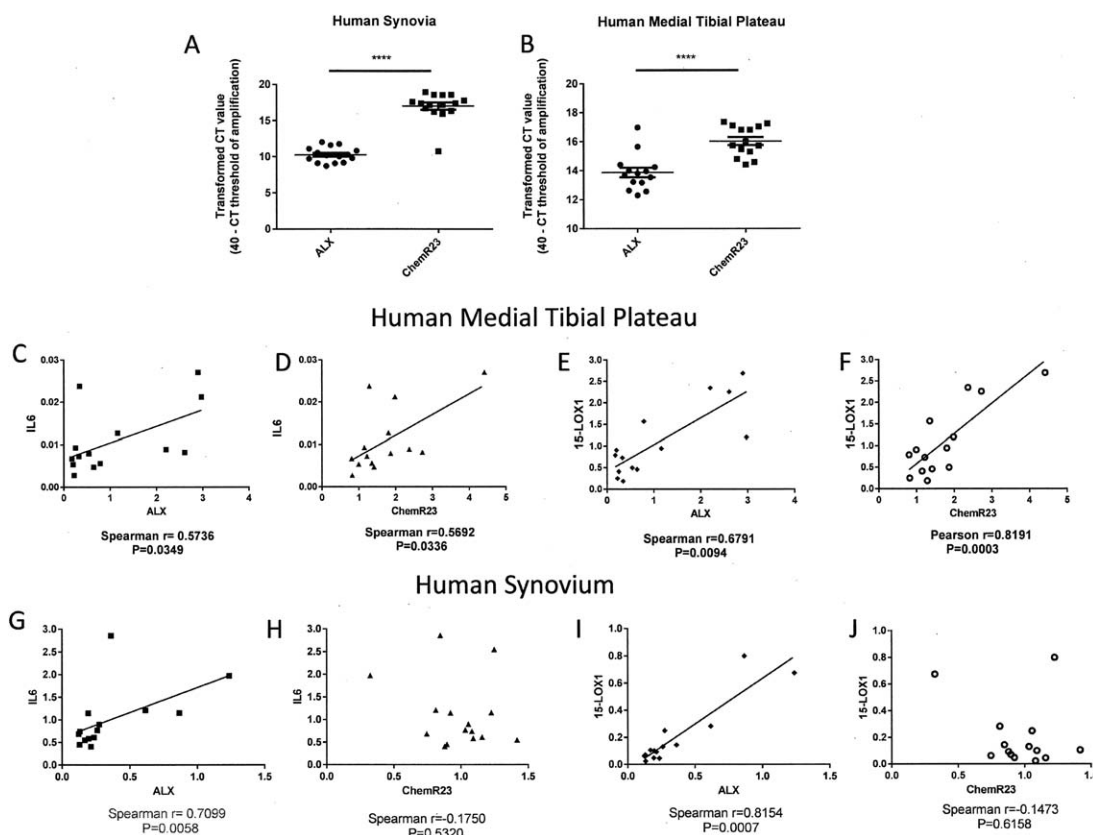


Figure 1. Expression of resolvins ALX and ChemR23 in human osteoarthritis (OA) joint tissue. **A** and **B**, Transformed C_t values for resolvins ALX and ChemR23 mRNA in synovium (**A**) and medial tibial plateau (**B**) specimens obtained from patients with end-stage OA. Expression of ChemR23 was significantly higher than that of ALX in both OA synovium ($n = 15$ specimens) (**A**) and medial tibial plateau ($n = 14$ specimens) (**B**), as shown by a larger transformed C_t value (maximum cycle number for run – cycle number at which exponential amplification occurs). Bars show the mean \pm SEM. **** = $P < 0.0001$ by unpaired t -test. **C–F**, Correlations of ALX and ChemR23 with the cytokine interleukin-6 (IL-6) and the enzyme 15-lipoxygenase 1 (15-LOX-1) in human medial tibial plateau tissue. **G–J**, Correlations of ALX and ChemR23 with IL-6 and 15-LOX-1 in human synovium.

collected at the time of TKR surgery was pulverized in liquid nitrogen, and RNA was extracted in TRI Reagent. RNA samples were kept in a -80°C freezer for future use (see Supplementary Methods, available on the *Arthritis & Rheumatology* web site at <http://onlinelibrary.wiley.com/doi/10.1002/art.40001/abstract>). Expression of target genes was quantified using previously described methods (26,28). Primers and probes were designed using Primer Express 3.0 software (Applied Biosystems) and synthesized by personnel at MWG Biotech, and minor groove binder probes were biosynthesized by personnel at Applied Biosystems (see Supplementary Methods).

Glial cell immunofluorescence analysis. Rats were killed by sodium pentobarbital overdose and transcardially perfused with saline and then 4% paraformaldehyde, pH 7.4 (Sigma). The lumbar spinal cord was removed, postfixed in 4% paraformaldehyde, and stored in 30% sucrose. The spinal cord was then sectioned, and immunohistochemical analysis was performed using mouse anti-glial fibrillary acidic protein (anti-GFAP) antibodies (1:100) (Fisher Scientific), as previously described (26) (see Supplementary Methods).

Histologic staining and scoring of knee joints. Cartilage histopathology was scored from 0 (normal) to 5 (severe

degeneration), and a total joint damage score (range 0–15) was obtained by combining the cartilage score with the score for joint involvement (range 0–3) (29). Synovial inflammation was graded on a scale of 0 (lining layer, 1–2 cells thick) to 3 (lining layer >9 cells thick and/or severe increase in cellularity), as previously described (29). Sections from the posterior half of the knee joints were dewaxed and recalcified with calcium chloride and magnesium chloride before tartrate-resistant acid phosphatase (TRAP) staining was conducted using a commercially available kit (F386A; Sigma-Aldrich). TRAP-positive osteoclasts were quantified as previously described (29) (see also Supplementary Methods, available on the *Arthritis & Rheumatology* web site at <http://onlinelibrary.wiley.com/doi/10.1002/art.40001/abstract>).

Statistical analysis. Data were analyzed with GraphPad Prism version 5 or 6 and are presented as the mean \pm SEM. Behavioral data were analyzed by two-way analysis of variance (ANOVA) with Bonferroni post hoc correction. Histologic scoring was analyzed by one-way ANOVA with Bonferroni post hoc test or by Kruskal-Wallis ANOVA followed by Dunn's post hoc test for nonparametric data. Gene expression levels were analyzed by unpaired t -test (parametric data) or Mann-Whitney test (nonparametric data). Correlations between gene expression of resolvins

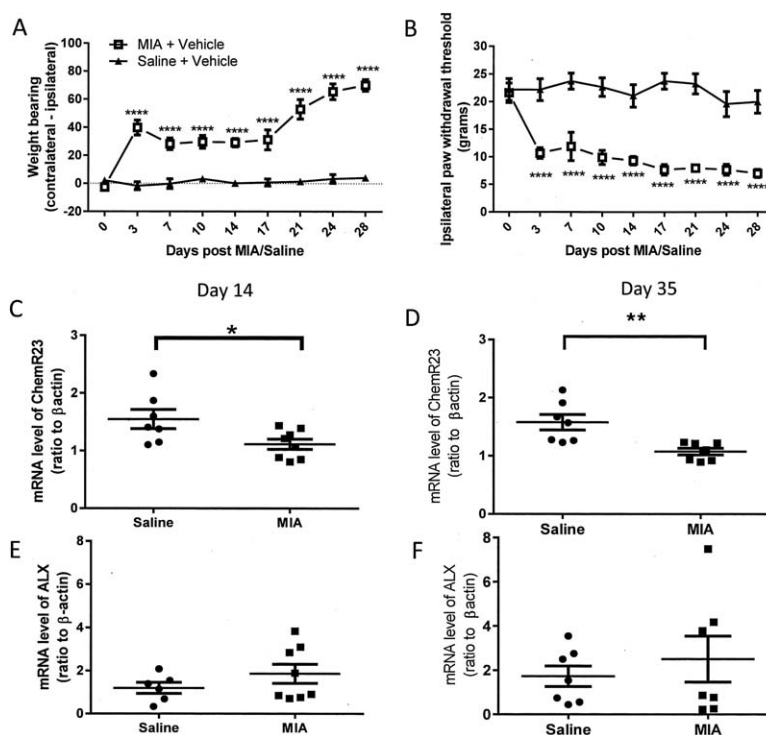


Figure 2. Expression of resolvin receptors ALX and ChemR23 in rat osteoarthritis (OA) joint tissue. **A** and **B**, Significant weight-bearing asymmetry (**A**) and decreased ipsilateral paw withdrawal thresholds (**B**) following intraarticular injection of monosodium iodoacetate (MIA) into the knee joints (MIA-treated rats) compared with saline-treated control rats ($n = 8$ per group). Values are the mean \pm SEM. **** = $P < 0.0001$ versus control, by two-way analysis of variance with Bonferroni's post hoc test. **C** and **D**, Decreased synovial expression of ChemR23 in MIA-treated rats compared with saline-treated control rats on day 14 (**C**) and day 35 (**D**). **E** and **F**, Comparable expression of ALX in the synovium of MIA-treated rats and saline-treated rats on day 14 (**E**) and day 35 (**F**) ($n = 7$ –8 per group). Bars in **C**–**F** show the mean \pm SEM. * = $P < 0.05$; ** = $P < 0.01$ by unpaired t -test.

receptors and pain behavior or genes of interest were analyzed using Pearson's correlation coefficient (parametric data) or Spearman's correlation coefficient (nonparametric data) analysis. For immunofluorescence analysis, data were analyzed by one-way ANOVA with Bonferroni post hoc test. Correlations between spinal GFAP expression and weight-bearing asymmetry and the ipsilateral paw withdrawal threshold were determined by a Spearman's correlation.

RESULTS

Expression of ChemR23 and ALX messenger RNA (mRNA) in the OA joint. Both ALX and ChemR23 were present in human synovium and medial tibial plateau bone obtained following TKR surgery for OA (Figures 1A and B). For the synovium, there was an approximate 6- C_t difference between ChemR23 and ALX, and for the medial tibial plateau bone there was a 2- C_t difference, indicating higher expression of ChemR23 compared with ALX in both tissues. Given the role of these receptors in regulating inflammatory signaling, it is noteworthy that the expression of both ChemR23 and ALX was positively correlated with mRNA expression of IL-6 in the medial tibial plateau bone

(Figures 1C and D). Expression of both ChemR23 and ALX was also positively correlated with expression of the enzyme 15-lipoxygenase 1 (15-LOX-1) in the medial tibial plateau bone (Figures 1E and F). In the synovium, correlations were less robust. Expression of ALX but not ChemR23 was positively correlated with IL-6 expression (Figures 1G and H), and expression of ALX was also positively correlated with 15-LOX-1 expression (Figures 1I and J). There was no correlation between body mass index (BMI) or age with expression of ALX, ChemR23, or any other genes studied in the synovium of OA patients (data not shown). Analysis of the correlation of BMI and age with expression of selected genes in medial tibial plateau bone from OA patients revealed a significant negative correlation between BMI and the expression of TNF. There was a significant negative correlation between age and expression of ChemR23 and 15-LOX-1 (data not shown).

The preclinical MIA model of OA pain was associated with marked weight-bearing asymmetry ($P < 0.0001$ versus saline + vehicle) (Figure 2A). In addition, MIA-induced OA pain was associated with reductions in ipsilateral paw

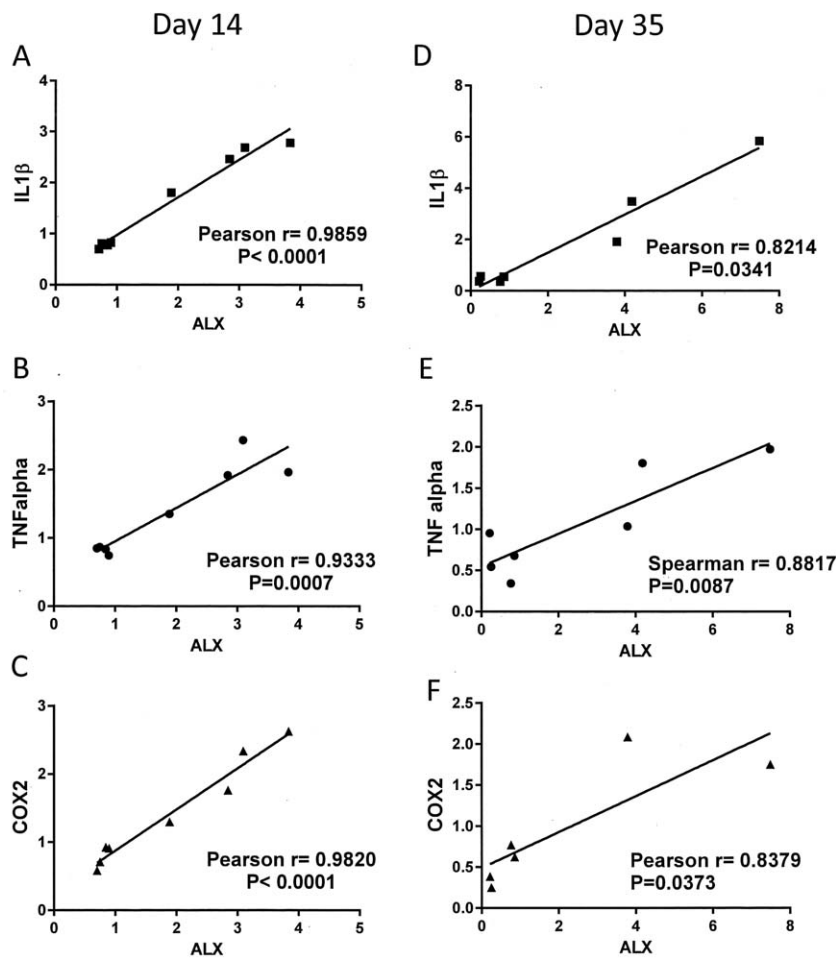


Figure 3. Correlations between synovial expression of ALX and markers of inflammation in rat synovium. Significant correlations between ALX expression and synovial expression of interleukin-1 β (IL-1 β), tumor necrosis factor (TNF), and cyclooxygenase 2 (COX-2) on day 14 (A–C) and day 35 (D–F) in monosodium iodoacetate-treated rats ($n = 7$) were found.

withdrawal thresholds ($P < 0.0001$ versus saline + vehicle) (Figure 2B), as previously described (25). Consistent with the clinical data, synovium from saline-treated (control) rats expressed both ChemR23 and ALX (Figures 2C–F). There was a significant reduction in ChemR23 expression in the synovium at both the earlier (day 14) (Figure 2C) and later (day 35) (Figure 2D) time points in MIA-treated animals compared with saline-treated controls. Synovial expression of ALX was unaltered in MIA-injected rats compared to saline-treated rats at either time point studied (Figures 2E and F).

Consistent with the clinical data, there was a trend toward a correlation between ALX and IL-6 expression (results not shown) at 14 days after induction of the model ($r = 0.6826$, $P = 0.0621$). At this time point, synovial ALX expression was correlated with IL-1 β , TNF, and COX-2 expression (Figures 3A–C). At the later time point, synovial ALX expression was correlated with IL-1 β , TNF, and

COX-2 expression in the synovium (Figures 3D–F). There were no significant correlations between ALX expression and IL-6, IL-1 β , TNF, and COX-2 expression in the synovium of control (saline-treated) rats (data not shown). There were no significant correlations between synovial expression of ChemR23 and IL-1 β , TNF, and COX-2 in the MIA-induced model of OA at either time point (data not shown).

The number of ALX-positive and ChemR23-positive cells in the synovium was compared in the MIA-treated rats (day 28 after the MIA injection) and saline-treated controls. The number of DAPI-positive nuclei, ED1/CD68-positive cells, and the number of ALX-positive and ChemR23-positive cells in synovial sections was evaluated. The number of DAPI-positive cells was increased ($P < 0.01$) in the synovium of rats with MIA-induced OA compared with saline-injected control rats (see

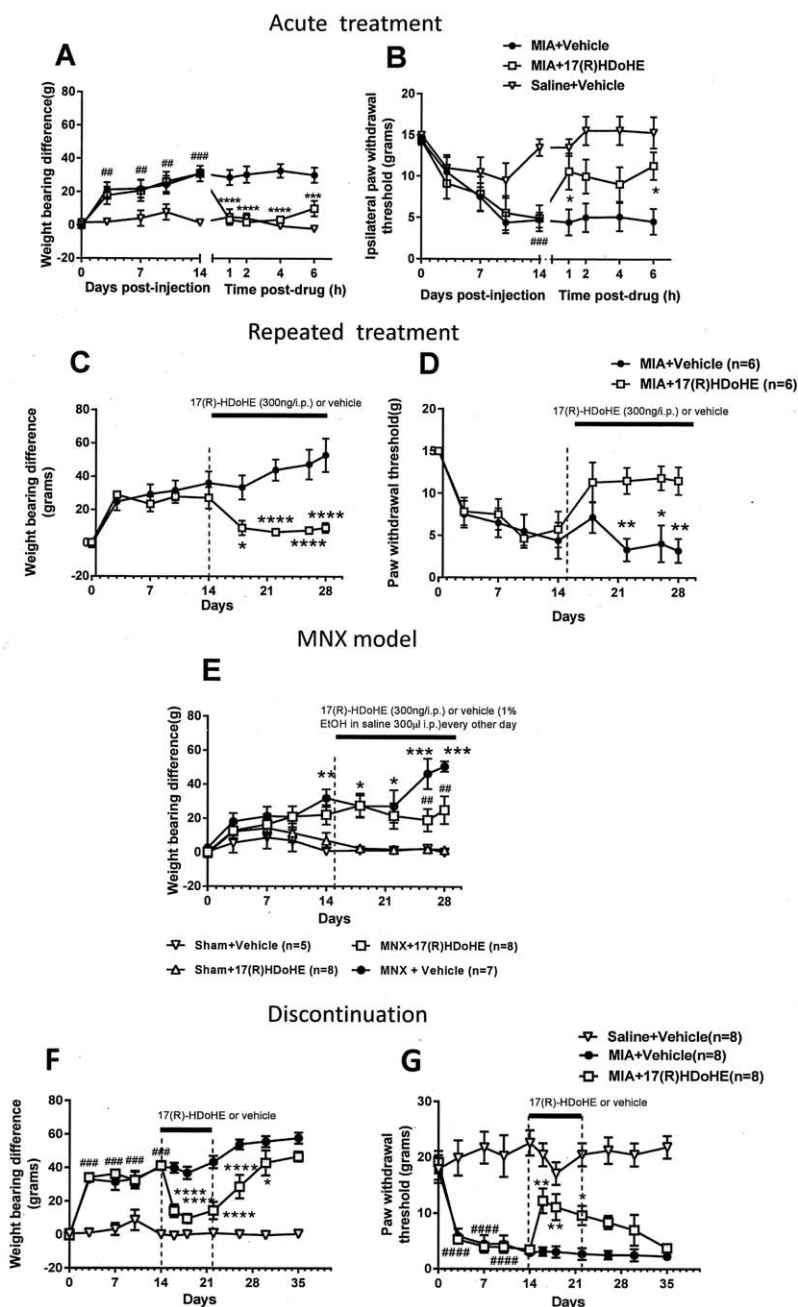


Figure 4. Inhibition of pain behavior by the D series resolvins precursor 17(R)-hydroxy-docosahexaenoic acid (17[R]-HDoHE). **A** and **B**, Attenuated weight-bearing asymmetry (**A**) and decreased ipsilateral hind paw withdrawal thresholds (**B**) 14 days after model induction in rats treated with monosodium iodoacetate (MIA) + 17(R)-HDoHE compared to MIA-injected vehicle-treated rats. Bars show the mean \pm SEM ($n = 8$ per group). $## = P < 0.01$; $### = P < 0.001$ versus saline + vehicle. $* = P < 0.05$; $*** = P < 0.001$; $**** = P < 0.0001$ versus MIA + vehicle, by two-way analysis of variance (ANOVA) with Bonferroni's post hoc test. **C** and **D**, Sustained inhibition of weight-bearing asymmetry (**C**) and decreased paw withdrawal thresholds (**D**) from day 14 to day 28 following repeated administration of 17(R)-HDoHE in rats treated with MIA compared with rats treated with MIA + vehicle. Bars show the mean \pm SEM. $* = P < 0.05$; $** = P < 0.01$; $**** = P < 0.0001$ versus MIA + vehicle, by two-way ANOVA with Bonferroni's post hoc test. **E**, Attenuated weight-bearing asymmetry in rats with medial meniscal transection (MNX)-induced osteoarthritis pain treated with repeated administration of 17(R)-HDoHE compared with those treated with vehicle. Bars show mean \pm SEM. $* = P < 0.05$; $** = P < 0.01$; $*** = P < 0.001$ versus sham + vehicle. $## = P < 0.01$ versus MNX + vehicle, by two-way ANOVA with Bonferroni's post hoc test. **F** and **G**, Gradual return of weight-bearing asymmetry and decreased hind paw withdrawal thresholds within 7 days following cessation of 7-day treatment with 17(R)-HDoHE. Bars show the mean \pm SEM. $### = P < 0.001$; $#### = P < 0.0001$ versus saline + vehicle. $* = P < 0.05$; $** = P < 0.01$; $**** = P < 0.0001$ versus MIA + vehicle, by two-way ANOVA with Bonferroni's post hoc test. Values are the mean \pm SEM. EtOH = ethanol.

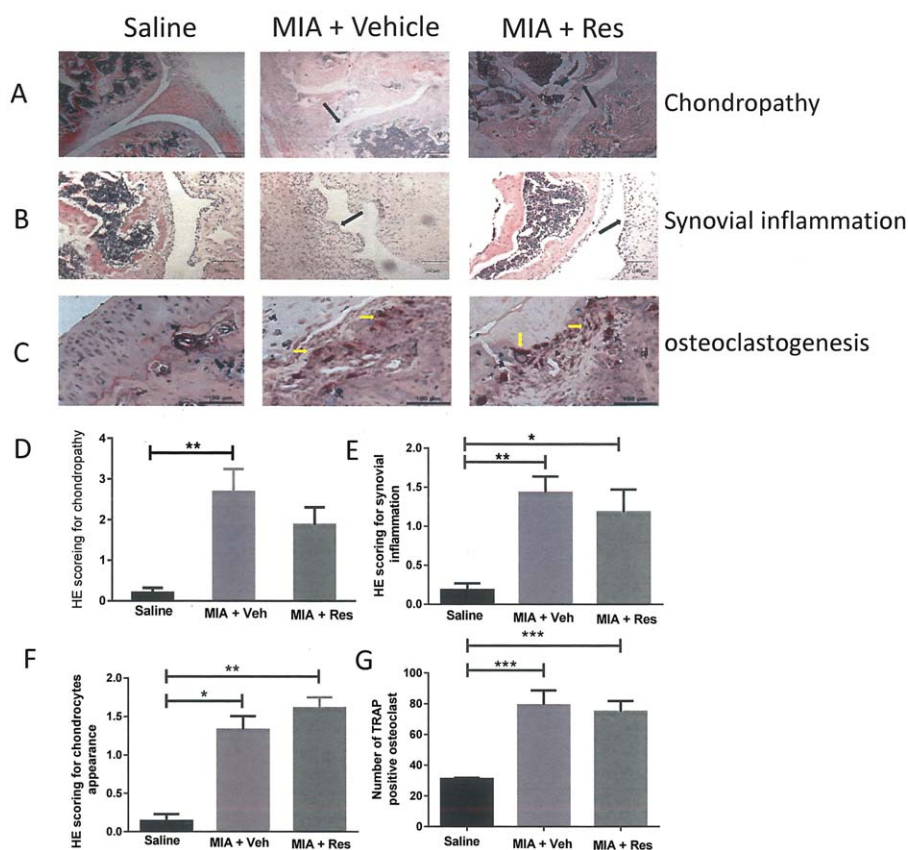


Figure 5. No alteration of osteoarthritis joint pathology by 17(R)-HDoHE (Res). **A–C**, Representative images of hematoxylin and eosin (H&E)-stained knee joint sections from rats treated with saline, MIA + vehicle (Veh), or MIA + 17(R)-HDoHE. **A**, Chondropathy. Bars = 500 μm . **B**, Synovial inflammation. Bars = 100 μm . **C**, Osteoclastogenesis. Bars = 100 μm . **Black arrows** indicate areas of chondropathy and synovial inflammation; **yellow arrows** indicate osteoclastogenesis. **D–G**, Significant joint pathology at 28 days in rats treated with intraarticular injections of MIA compared with saline-treated rats. Repeated administration of 17(R)-HDoHE from day 14 to day 28 did not alter the chondropathy score (**D**), synovial inflammation (**E**), chondrocyte appearance (**F**), or number of tartrate-resistant acid phosphatase (TRAP)-positive osteoclasts (**G**) in the MIA-treated rats. Bars show the mean \pm SEM. * = $P < 0.05$; ** = $P < 0.01$; *** = $P < 0.001$ by one-way ANOVA with Bonferroni's post hoc test (parametric data) or Kruskal-Wallis test with Dunn's post hoc test (nonparametric data). See Figure 4 for other definitions.

Supplementary Figures 1A and B, available on the *Arthritis & Rheumatology* web site at <http://onlinelibrary.wiley.com/doi/10.1002/art.40001/abstract>). In addition, the number of ED1-positive cells (see Supplementary Figures 1A and C) was also increased in the rats with MIA-induced OA ($P < 0.005$), which is indicative of the likely infiltration of ED1-positive macrophages in this model. Despite the increase in the number of macrophages in the synovium of rats with MIA-induced OA pain, the number of ALX-positive and ChemR23-positive cells in the synovium was significantly reduced in MIA-treated rats compared with saline-treated rats (see Supplementary Figures 1A, D, and E) ($P < 0.05$ for both ALX and ChemR23).

In order to confirm that the antibody staining was not attributable to autofluorescence, we conducted negative control experiments with omission of the primary

antibodies (see Supplementary Figure 2, available on the *Arthritis & Rheumatology* web site at <http://onlinelibrary.wiley.com/doi/10.1002/art.40001/abstract>), in which positively labeled cells were not evident either visually or by velocity analysis. We attempted colocalization experiments for ED1-positive cells and ALX and ChemR23, but unfortunately we were unable to obtain sufficient quality of staining when these antibodies were applied to synovial sections for analysis.

Reversal of MIA- and MNX-induced OA pain by the D series precursor 17(R)-HDoHE. In a series of intervention studies, we evaluated the ability of systemic administration of 17(R)-HDoHE to reverse pain behavior in 2 models of OA. Systemic administration produced a pronounced and complete reversal of MIA-induced weight-bearing asymmetry and restored ipsilateral paw withdrawal

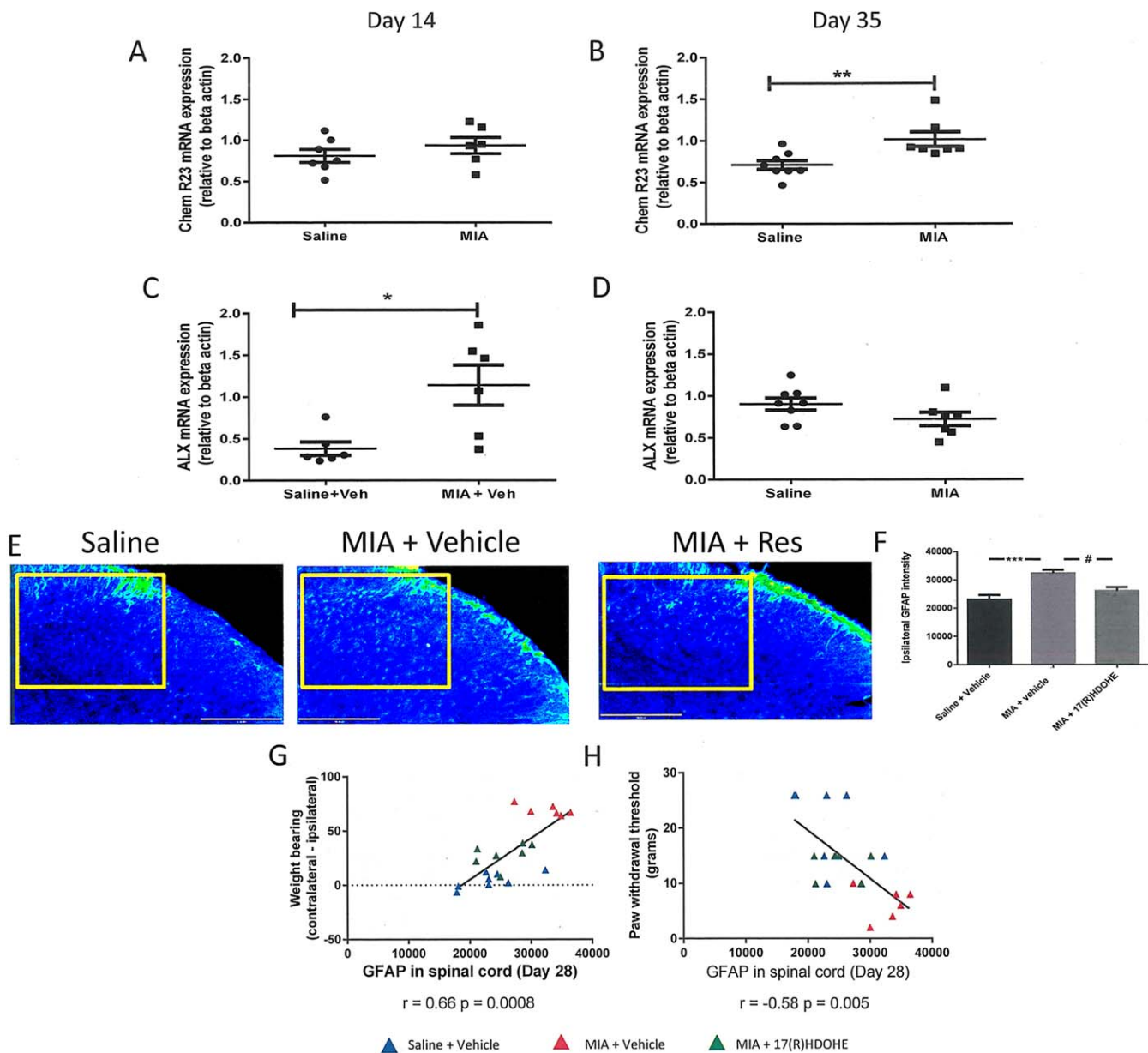


Figure 6. Expression of the resolvin receptors in the spinal cord. **A** and **B**, ChemR23 expression in the ipsilateral dorsal horn of the lumbar spinal cord (L3–L5) on day 14 (**A**) and day 35 (**B**) in MIA-treated rats compared with saline-treated rats. **C** and **D**, ALX expression in the ipsilateral dorsal horn of the lumbar spinal cord (L3–L5) on day 14 (**C**) and day 35 (**D**) in MIA-treated rats compared with saline-treated rats. Bars show the mean \pm SEM ($n = 5\text{--}6$ per group). $* = P < 0.05$; $** = P < 0.01$ by unpaired *t*-test. **E**, Anti-gliofibrillary acidic protein (GFAP) immunofluorescence in the ipsilateral L4 dorsal horn of the spinal cord 28 days following induction of the MIA model of OA pain, indicative of increased astrocyte reactivity. Repeated systemic treatment with 17(R)-HDoHE (300 ng every other day from day 14 to day 28 after model induction) resulted in a significant decrease in MIA-induced GFAP immunofluorescence. The boxed area shows the area evaluated for GFAP quantification. **F**, Quantification of GFAP fluorescence. Bars show the mean \pm SEM ($n = 7\text{--}8$ rats per group). $**** = P < 0.001$; $\# = P < 0.05$ by one-way ANOVA. **G**, Positive correlation between GFAP expression in the ipsilateral dorsal horn of the spinal cord and weight-bearing asymmetry in all of the treatment groups. **H**, Negative correlation between GFAP expression in the ipsilateral dorsal horn of the spinal cord and the paw withdrawal threshold in all of the treatment groups. See Figure 4 for other definitions.

thresholds toward control values at 1 hour after administration; these effects lasted for 6 hours (Figures 4A and B). Importantly, the inhibitory effects of 17(R)-HDoHE on

both weight-bearing asymmetry and hind paw withdrawal thresholds were sustained following repeated administration of 17(R)-HDoHE for 14 days (Figures 4C and D);

there was no evidence of tolerance to this analgesic effect. To consolidate the evidence that these inhibitory effects of the resolvin precursor on MIA-induced pain behavior has translational relevance, the effects of 17(R)-HDoHE on pain behavior were also evaluated in the MNX-induced model of OA. In this analysis, systemic administration of 17(R)-HDoHE (300 ng intraperitoneally every other day from day 14 after model induction) significantly halted further increases in MNX-induced weight-bearing asymmetry (Figure 4E).

The final series of pharmacologic experiments determined the extent to which 17(R)-HDoHE administration altered pain behavior once treatment had ceased. Following a 7-day treatment protocol with 17(R)-HDoHE (days 14–22 after MIA/saline injection), pain behavior was assessed for a further 13 days. It was evident that the analgesic effects of 17(R)-HDoHE were sustained over a short period of time once treatment had ceased, and then pain behavior returned to levels observed in saline-treated rats with MIA-induced OA pain (Figures 4F and G).

To further investigate the potential mechanisms underlying the effects of 17(R)-HDoHE on OA-induced pain behavior, the effects of repeated treatment with 17(R)-HDoHE on joint pathology were determined (Figures 5A–C). Intraarticular injection of MIA was associated with a significant increase in chondropathy, synovitis, and chondrocyte appearance and increased numbers of subchondral osteoclasts (Figures 5D–G). Following repeated administration of 17(R)-HDoHE (300 ng in 300 μ l every other day from day 14 to day 28) there were no significant changes in any of these features of OA joint pathology (Figures 5D–G). Similarly, repeated treatment with 17(R)-HDoHE did not alter MNX-induced joint pathology (data not shown).

Spinal effects of 17(R)-HDoHE correlated with behavioral analgesia. Given the lack of effect of 17(R)-HDoHE on joint pathology in 2 models of OA pain, we investigated potential spinal mechanisms underlying these effects. ChemR23 expression in the spinal cord on day 14 in MIA-treated rats was comparable with that in saline-treated controls (Figure 6A); however, expression was increased on day 35 in MIA-treated rats compared with saline-treated controls (Figure 6B). The expression of ALX in the ipsilateral dorsal horn of the spinal cord was increased in MIA-treated rats compared with saline-treated rats on day 14 (Figure 6C), while on day 35 there was no difference in spinal ALX expression between MIA-treated and saline-treated rats (Figure 6D).

We previously reported a significant increase in GFAP immunofluorescence, a marker for astrogliosis, in the spinal cord at later time points in the MIA-induced model of OA (25). Consistent with previous findings,

GFAP immunofluorescence was significantly increased in the ipsilateral dorsal horn (Figures 6E and F) but not the contralateral dorsal horn (data not shown) of MIA-treated rats that received vehicle, compared with saline-treated controls. Repeated systemic administration of 17(R)-HDoHE (300 ng in 300 μ l every other day from day 14 to day 28) significantly inhibited GFAP immunofluorescence in the ipsilateral dorsal horn of the spinal cord in MIA-treated rats, compared with vehicle-treated rats with MIA-induced OA pain (Figures 6E and F). Correlation analysis revealed that spinal GFAP expression was positively correlated with weight-bearing asymmetry (Figure 6G) and negatively correlated with ipsilateral paw withdrawal thresholds (Figure 6H).

Liquid chromatography tandem mass spectrometry (LC-MS/MS) quantitative analysis of resolvins and 17(R)-HdoHE. Plasma levels of 45 oxylipins, including arachidonic acid, RvD1, RvD2, and the precursor 17(R)-HDoHE were quantified 150 minutes following systemic administration of 17(R)-HDoHE in MIA-treated rats, vehicle-treated rats, and saline-treated controls. Levels of arachidonic acid were not altered by systemic administration of 17(R)-HDoHE (see Supplementary Figures 3A and D, available on the *Arthritis & Rheumatology* web site at <http://onlinelibrary.wiley.com/doi/10.1002/art.40001/abstract>). As expected at the time point studied, plasma levels of 17(R)-HDoHE were not altered following 17(R)-HDoHE pretreatment (see Supplementary Figures 3B and E), but levels of RvD2 were significantly increased in 17(R)-HDoHE-treated rats with MIA-induced OA compared with vehicle-treated rats with MIA-induced OA (see Supplementary Figures 3C and F). Although there were no significant differences in the group data for plasma levels of RvD1, this lipid was detected in a larger number of samples following 17(R)-HDoHE treatment (5 of 8 samples) compared with those that received vehicle (3 of 8). Of the remaining oxylipins quantified, only 9-oxo-10E,12Z-octadecadienoic acid (9-oxoODE) and 13-oxoODE were significantly increased in the group of rats with MIA-induced OA treated with 17(R)-HDoHE compared with the group that received saline plus vehicle (data not shown).

DISCUSSION

Herein we report that the resolvin receptors ALX and ChemR23 are expressed at the mRNA level in both the synovium and tibial plateau of OA patients. ALX expression was positively correlated with expression of IL-6, which is a clinically relevant knee pain biomarker in patients with early OA and those with advanced-stage knee OA (30), and positively correlated with expression of 15-LOX-1, a key enzyme involved in D series resolvin generation, in both OA synovium and medial tibial plateau

bone. Associations between ChemR23, 15-LOX-1, and IL-6 expression were less consistent for both tissues. The enzyme 15-LOX-1 is involved in the biosynthesis of D series resolvins from DHA but not the production of E series resolvins from EPA; therefore, correlations between 15-LOX-1 and ChemR23 may reflect the more general role of 15-LOX-1 in inflammatory pathways. Although correlations between these inflammatory mediators and resolvin receptor expression do not necessarily reflect a causal relationship, they do support the need for further investigation of the role of the resolvin system in OA mechanisms. Due to the lack of availability of fresh non-OA knee synovium and tibial plateau bone, we were unable to evaluate whether expression of ALX and ChemR23 is altered in end-stage OA. To overcome this inevitable hurdle of clinical research, preclinical studies using well-established models of OA pain in the rodent were undertaken.

Both ALX and ChemR23 were present in control rat synovium at the early and late time points in the model of MIA-induced OA pain. The impact of this model of OA on the expression of these receptors differed. Expression of ChemR23 mRNA was reduced in the synovium at both the early and late time points in the MIA model of OA. In contrast, synovial expression of ALX mRNA in MIA-injected rats remained stable and comparable with levels in saline-treated rats at both time points in the model of MIA-induced OA pain. Synovial expression of ALX mRNA in the MIA-induced model of OA pain was positively correlated with key inflammatory genes (TNF, IL-1 β , IL-6, and COX-2), which is consistent with the presence of synovial inflammation in this model of OA pain, described herein and in previous studies (31–33), and the expression of ALX by neutrophils, macrophages, and fibroblast-like synoviocytes (34).

In addition to the findings of the gene expression studies, we also demonstrated an increased number of ED1-positive cells in the synovium of rats with MIA-induced pain compared with control rats, reflecting a likely increase in macrophage infiltration. These events were associated with a decrease in the number of ChemR23-positive and ALX-positive cells in the synovium of MIA-treated rats compared with controls. Thus, there was a consistent direction of effect for ChemR23 mRNA and protein. In contrast, ALX mRNA expression was not altered, but the numbers of ALX-positive cells were decreased in the synovium of MIA-treated rats, which may reflect posttranslational changes in this receptor.

Systemic administration of the D series resolvin precursor 17(R)-HDoHE produced robust inhibition of established pain behavior in both the chemically induced and surgically induced OA pain models. Systemic treatment with a single dose of 17(R)-HDoHE rapidly reversed

established weight-bearing asymmetry, and this reversal was evident 1 hour posttreatment and was sustained for 6 hours. LC-MS/MS analysis of plasma confirmed that this treatment significantly increased plasma levels of RvD2 and increased the number of samples in which RvD1 was detectable. The dose of 17(R)-HDoHE studied was based on the comprehensive pharmacologic evaluation of 17(R)-HDoHE in a model of inflammatory arthritis (17). Consistent with this previous study, we observed that a very low dose of 17(R)-HDoHE has beneficial effects on pain behavior, and that repeated treatment with 17(R)-HDoHE has a sustained inhibitory effect on pain behavior over a 2-week period in both the chemically induced and surgically induced models of OA pain. Although there were subtle differences in the rapidity of onset and magnitude of the inhibitory effects of 17(R)-HDoHE between the 2 models of OA pain, overall this treatment had a comparable inhibitory effect in the 2 models. Unlike opioid-based analgesics, sustained treatment with 17(R)-HDoHE did not lead to tolerance.

To further investigate the underlying mechanisms leading to the beneficial effects of 17(R)-HDoHE, the effects of repeated treatment on joint pathology were quantified in the model of MIA-induced pain. Consistent with previous studies (26,35–37) and the key clinical features of OA, the model of MIA-induced OA was associated with significant cartilage damage, synovial inflammation, and increased numbers of subchondral osteoclasts. Despite the robust analgesic effects of 17(R)-HDoHE, this treatment did not alter any of the features of knee joint pathology. This was also the case in the model of MNX-induced OA pain and joint pathology. This observation is consistent with our demonstration that the numbers of ALX-positive cells were reduced in the synovium of rats with MIA-induced OA pain compared with saline-treated controls, which is likely to limit/reduce any possible effects of 17(R)-HDoHE at this level. We previously showed that treatments that act to reduce osteoclast function can alter the progression of joint pathology under identical experimental conditions (29). Unlike RvE1, which can inhibit osteoclasts and bone resorption (38) and protects against bone loss (39,40), evidence for a role of RvD1 in bone modulation is sparse. It is feasible, however, that a higher dose of 17(R)-HDoHE may alter pathologic knee changes seen in these models of OA. Overall, our *in vivo* data demonstrate that 17(R)-HDoHE can robustly block pain behavior in the MIA model of OA in the face of overt joint damage and synovial inflammation.

Once treatment with 17(R)-HDoHE was stopped, pain behavior was blocked for an additional 5–7 days, suggesting that augmentation of the resolvin system has longer-term inhibitory effects on nociceptive signaling, which may

represent alterations in both channel activity and signaling pathways. Chronic pain states are often associated with changes in the spinal signaling pathways and increased excitability of spinal neurones, coupled with increased activation of proinflammatory signaling pathways and changes in the activation state of microglia and astrocytes (41).

RvD1 is known to suppress TRPA-1, TRPV-3, and TRPV-4 channel activity in primary sensory fibers (18,21); therefore, systemic administration of 17(R)-HDoHE may act to reduce sensory nerve activity arising from the damaged knee joint. It is noteworthy that deletion of TRPA-1 attenuates joint pathology and pain behavior in the mouse model of MIA-induced OA (42). It is possible that 17(R)-HDoHE may still have effects at the level of the joint by activating ALX receptors on synovial cells and possibly reducing release of synovium-derived nerve sensitization factors such as NGF (43).

Direct spinal administration of RvD1 inhibited evoked pain behavior in models of acute and chronic pain (18,21,22); similarly, spinal administration of 17(R)-HDoHE attenuated inflammation-induced mechanical hypersensitivity (22). Although the spinal mechanisms underlying the effects of RvD1 are not fully established, common pathways implicated include reductions in TNF release (22) and inhibition of ERK signaling (21). In the current study, immunohistochemical analysis revealed that both ChemR23 and ALX expression in the ipsilateral dorsal horn of the spinal cord is either increased or unaltered in rats with MIA-induced OA pain compared with that in saline-treated controls at the 2 time points studied, providing a putative spinal site of action for the resolvins in this model of OA. It is possible that 17(R)-HDoHE may still have effects at the level of the joint by activating ALX receptors on synovial cells and possibly reducing release of synovium-derived nerve sensitization factors such as NGF (43).

We previously demonstrated a significant increase in GFAP immunofluorescence, indicative of astrogliosis and a marker of central sensitization, in the ipsilateral dorsal horn of the spinal cord at later time points in the model of MIA-induced OA pain (25). In the current study, repeated treatment with 17(R)-HDoHE from day 14 onward resulted in significant blockade of spinal astrogliosis in the model of MIA-induced OA pain at the later time point (day 28 after induction of the model), and spinal GFAP expression at this time was correlated with pain behavior. We previously showed that post mortem knee chondropathy scores are significantly and positively correlated with human spinal GFAP mRNA expression (26), confirming the clinical relevance of these spinal markers of central sensitization.

Astrogliosis is associated with numerous models of chronic pain (for review, see ref. 44) and is a proposed switch in the transition from acute to chronic pain mechanisms (45). The ability of 17(R)-HDoHE to inhibit spinal astrogliosis in preclinical models of OA, along with the clinical associations between joint damage and spinal GFAP expression, supports the need for further investigation of the therapeutic potential of the D series resolvins pathway. The mechanisms by which 17(R)-HDoHE inhibits astrogliosis may arise as a result of direct effects (although there is little evidence to date) or indirect effects on the spinal signaling pathways that lead to astrogliosis. In particular, activated microglia in the spinal cord play a fundamental role in the development of chronic pain mechanisms and are known to be activated 14–28 days following induction of the MIA model of OA (25), coinciding with the increase in expression of ALX in the ipsilateral spinal cord reported herein.

Microglia are known to express ALX (46,47), and activation of microglia in models of chronic pain states, including OA, is associated with increased levels of pERK (48), a known spinal target of 17(R)-HDoHE (21). In addition, the antiinflammatory and pro-resolution molecule lipoxin A₄ also signals through ALX (49), and increases in ALX expression seen in the spinal cord in the MIA model may indicate an enhanced antiinflammatory role of lipoxin A₄.

The results of this series of experiments demonstrate that receptors for both D series and E series resolvins are expressed at multiple sites within the human OA joint, and that the precursor for the D series resolvins reduced OA pain behavior and a key marker of central sensitization (astrocyte activation) associated with chronic pain. These effects, which were not subject to tolerance, at least over a 2-week period of treatment, likely arise from modulation of both nociceptive input arising from the arthritic joint and modulation of central nociceptive processing. Our findings support the need for further investigation of the therapeutic potential of this new class of analgesics for the treatment of OA pain. Future work could address whether combination treatments that use both 17(R)-HDoHE and an E series resolvins precursor such as hydroxy-eicosapentaenoic acid would produce superior analgesic efficacy and potential disease-modifying properties via the modulation of both resolvins signaling systems.

ACKNOWLEDGMENTS

We thank the Nottingham University Hospitals NHS Trust Biobank and all of the individuals who consented to provide synovium and medial tibial plateau tissue samples following total knee replacement surgery.

AUTHOR CONTRIBUTIONS

All authors were involved in drafting the article or revising it critically for important intellectual content, and all authors approved the final version to be published. Drs. Burston and Chapman had full access to all of the data in the study and take responsibility for the integrity of the data and the accuracy of the data analysis.

Study conception and design. Huang, Burston, Mapp, Bennett, Ravipati, Pousinis, Barrett, Scammell, Chapman.

Acquisition of data. Huang, Burston, Li, Ashraf, Mapp, Ravipati.

Analysis and interpretation of data. Huang, Burston, Li, Ashraf, Bennett, Ravipati, Pousinis, Barrett, Scammell, Chapman.

REFERENCES

- Glyn-Jones S, Palmer AJ, Agricola R, Price AJ, Vincent TL, Weinans H, et al. Osteoarthritis. *Lancet* 2015;386:376–87.
- Karsdal MA, Bay-Jensen AC, Lories RJ, Abramson S, Spector T, Pastoureau P, et al. The coupling of bone and cartilage turnover in osteoarthritis: opportunities for bone antiresorptives and anabolics as potential treatments? *Ann Rheum Dis* 2014;73:336–48.
- Murray CJ, Vos T, Lozano R, Naghavi M, Flaxman AD, Michaud C, et al. Disability-adjusted life years (DALYs) for 291 diseases and injuries in 21 regions, 1990–2010: a systematic analysis for the Global Burden of Disease Study 2010. *Lancet* 2012;380:2197–223.
- Felson DT, Chaisson CE, Hill CL, Totterman SM, Gale ME, Skinner KM, et al. The association of bone marrow lesions with pain in knee osteoarthritis. *Ann Intern Med* 2001;134:541–9.
- Arendt-Nielsen L, Skou ST, Nielsen TA, Petersen KK. Altered central sensitization and pain modulation in the CNS in chronic joint pain. *Curr Osteoporos Rep* 2015;13:225–34.
- Dakin H, Gray A, Fitzpatrick R, Maclennan G, Murray D, the KAT Trial Group. Rationing of total knee replacement: a cost-effectiveness analysis on a large trial data set. *BMJ Open* 2012;2:e000332.
- Serhan CN, Hong S, Gronert K, Colgan SP, Devchand PR, Mirick G, et al. Resolvins: a family of bioactive products of omega-3 fatty acid transformation circuits initiated by aspirin treatment that counter proinflammation signals. *J Exp Med* 2002;196:1025–37.
- Serhan CN, Clish CB, Brannon J, Colgan SP, Chiang N, Gronert K. Novel functional sets of lipid-derived mediators with antiinflammatory actions generated from omega-3 fatty acids via cyclooxygenase 2-nonsteroidal antiinflammatory drugs and transcellular processing. *J Exp Med* 2000;192:1197–204.
- Krishnamoorthy S, Recchiuti A, Chiang N, Yacoubian S, Lee CH, Yang R, et al. Resolvin D1 binds human phagocytes with evidence for proresolving receptors. *Proc Natl Acad Sci U S A* 2010;107:1660–5.
- Dalli J, Winkler JW, Colas RA, Arnardottir H, Cheng CY, Chiang N, et al. Resolvin D3 and aspirin-triggered resolvin D3 are potent immunoresolvents. *Chem Biol* 2013;20:188–201.
- Chiang N, Fredman G, Backhed F, Oh SF, Vickery T, Schmidt BA, et al. Infection regulates pro-resolving mediators that lower antibiotic requirements. *Nature* 2012;484:524–8.
- Arita M, Bianchini F, Aliberti J, Sher A, Chiang N, Hong S, et al. Stereochemical assignment, antiinflammatory properties, and receptor for the omega-3 lipid mediator resolvin E1. *J Exp Med* 2005;201:713–22.
- Arita M, Ohira T, Sun YP, Elangovan S, Chiang N, Serhan CN. Resolvin E1 selectively interacts with leukotriene B4 receptor BLT1 and ChemR23. *J Immunol* 2007;178:3912–7.
- Serhan CN, Petasis NA. Resolvins and protectins in inflammation resolution. *Chem Rev* 2011;111:5922–43.
- Ji RR, Xu ZZ, Strichartz G, Serhan CN. Emerging roles of resolvins in the resolution of inflammation and pain. *Trends Neurosci* 2011;34:599–609.
- Sungjae Yoo, Lim JY, Hwang SW. Resolvins: endogenously-generated potent painkilling substances and their therapeutic perspectives. *Curr Neuropharmacol* 2013;11:664–76.
- Lima-Garcia JF, Dutra RC, da Silva K, Motta EM, Campos MM, Calixto JB. The precursor of resolvin D series and aspirin-triggered resolvin D1 display anti-hyperalgesic properties in adjuvant-induced arthritis in rats. *Br J Pharmacol* 2011;164:278–93.
- Bang S, Yoo S, Yang TJ, Cho H, Kim YG, Hwang SW. Resolvin D1 attenuates activation of sensory transient receptor potential channels leading to multiple anti-nociception. *Br J Pharmacol* 2010;161:707–20.
- Bang S, Yoo S, Yang TJ, Cho H, Hwang SW. 17(R)-resolvin D1 specifically inhibits transient receptor potential ion channel vanilloid 3 leading to peripheral antinociception. *Br J Pharmacol* 2012;165:683–92.
- Xu ZZ, Berta T, Ji RR. Resolvin E1 inhibits neuropathic pain and spinal cord microglial activation following peripheral nerve injury. *J Neuroimmune Pharmacol* 2012;8:37–41.
- Xu ZZ, Zhang L, Liu T, Park JY, Berta T, Yang R, et al. Resolvins RvE1 and RvD1 attenuate inflammatory pain via central and peripheral actions. *Nat Med* 2010;16:592–7.
- Abdelmoaty S, Wigerblad G, Bas DB, Codeluppi S, Fernandez-Zafra T, El-Awady el-S, et al. Spinal actions of lipoxin A4 and 17(R)-resolvin D1 attenuate inflammation-induced mechanical hypersensitivity and spinal TNF release. *PLoS One* 2013;8:e75543.
- Feng QX, Feng F, Feng XY, Li SJ, Wang SQ, Liu ZX, et al. Resolvin D1 reverses chronic pancreatitis-induced mechanical allodynia, phosphorylation of NMDA receptors, and cytokines expression in the thoracic spinal dorsal horn. *BMC Gastroenterol* 2012;12:148.
- Tang H, Liu Y, Yan C, Petasis NA, Serhan CN, Gao H. Protective actions of aspirin-triggered (17R) resolvin D1 and its analogue, 17R-hydroxy-19-para-fluorophenoxy-resolvin D1 methyl ester, in C5a-dependent IgG immune complex-induced inflammation and lung injury. *J Immunol* 2014;193:3769–78.
- Sagar DR, Burston JJ, Hathway GJ, Woodhams SG, Pearson RG, Bennett AJ, et al. The contribution of spinal glial cells to chronic pain behaviour in the monosodium iodoacetate model of osteoarthritic pain. *Mol Pain* 2011;7:88.
- Mapp PI, Sagar DR, Ashraf S, Burston JJ, Suri S, Chapman V, et al. Differences in structural and pain phenotypes in the sodium monoiodoacetate and meniscal transection models of osteoarthritis. *Osteoarthritis Cartilage* 2013;21:1336–45.
- Sagar DR, Nwosu L, Walsh DA, Chapman V. Dissecting the contribution of knee joint NGF to spinal nociceptive sensitization in a model of OA pain in the rat. *Osteoarthritis Cartilage* 2015;23:906–13.
- Erhuma A, Salter AM, Sculley DV, Langley-Evans SC, Bennett A. Prenatal exposure to a low protein diet programmes disordered regulation of lipid metabolism in the ageing rat. *Am J Physiol Endocrinol Metab* 2007;292:1702–14.
- Sagar DR, Ashraf S, Xu L, Burston JJ, Menhinick MR, Poulter CL, et al. Osteoprotegerin reduces the development of pain behaviour and joint pathology in a model of osteoarthritis. *Ann Rheum Dis* 2014;73:1558–65.
- Shimura Y, Kurosawa H, Sugawara Y, Tsuchiya M, Sawa M, Kaneko H, et al. The factors associated with pain severity in patients with knee osteoarthritis vary according to the radiographic disease severity: a cross-sectional study. *Osteoarthritis Cartilage* 2013;21:1179–84.
- Hulejova H, Baresova V, Klezl Z, Polanska M, Adam M, Senolt L. Increased level of cytokines and matrix metalloproteinases in osteoarthritic subchondral bone. *Cytokine* 2007;38:151–6.
- Venn G, Nietfeld JJ, Duits AJ, Brennan FM, Arner E, Covington M, et al. Elevated synovial fluid levels of interleukin-6 and tumor necrosis factor associated with early experimental canine osteoarthritis. *Arthritis Rheum* 1993;36:819–26.
- Alvarez-Soria MA, Herrero-Beaumont G, Moreno-Rubio J, Calvo E, Santillana J, Egido J, et al. Long-term NSAID

- treatment directly decreases COX-2 and mPGES-1 production in the articular cartilage of patients with osteoarthritis. *Osteoarthritis Cartilage* 2008;16:1484–93.
34. Fiore S, Antico G, Aloman M, Sodin-Semrl S. Lipoxin A4 biology in the human synovium: role of the ALX signaling pathways in modulation of inflammatory arthritis. *Prostaglandins Leukot Essent Fatty Acids* 2005;73:189–96.
 35. Guzman RE, Evans MG, Bove S, Morenko B, Kilgore K. Monoiodoacetate-induced histologic changes in subchondral bone and articular cartilage of rat femorotibial joints: an animal model of osteoarthritis. *Toxicol Pathol* 2003;31:619–24.
 36. Janusz MJ, Bendele AM, Brown KK, Taiwo YO, Hsieh L, Heitmeyer SA. Induction of osteoarthritis in the rat by surgical tear of the meniscus: inhibition of joint damage by a matrix metalloproteinase inhibitor. *Osteoarthritis Cartilage* 2002;10:785–91.
 37. Beyreuther B, Callizot N, Stohr T. Antinociceptive efficacy of lacosamide in the monosodium iodoacetate rat model for osteoarthritis pain. *Arthritis Res Ther* 2007;9:R14.
 38. Herrera BS, Ohira T, Gao L, Omori K, Yang R, Zhu M, et al. An endogenous regulator of inflammation, resolvins E1, modulates osteoclast differentiation and bone resorption. *Br J Pharmacol* 2008;155:1214–23.
 39. Gao L, Faibish D, Fredman G, Herrera BS, Chiang N, Serhan CN, et al. Resolvins E1 and chemokine-like receptor 1 mediate bone preservation. *J Immunol* 2013;190:689–94.
 40. Hasturk H, Kantarci A, Ohira T, Arita M, Ebrahimi N, Chiang N, et al. RvE1 protects from local inflammation and osteoclast-mediated bone destruction in periodontitis. *FASEB J* 2006;20:401–3.
 41. Scholz J, Woolf CJ. The neuropathic pain triad: neurons, immune cells and glia. *Nat Neurosci* 2007;10:1361–8.
 42. Moilanen LJ, Hamalainen M, Nummenmaa E, Ilmarinen P, Vuolteenaho K, Nieminen RM, et al. Monosodium iodoacetate-induced inflammation and joint pain are reduced in TRPA1 deficient mice: potential role of TRPA1 in osteoarthritis. *Osteoarthritis Cartilage* 2015;23:2017–26.
 43. Shutov LP, Warwick CA, Shi X, Gnanasekaran A, Shepherd AJ, Mohapatra DP, et al. The complement system component C5a produces thermal hyperalgesia via macrophage-to-nociceptor signaling that requires NGF and TRPV1. *J Neurosci* 2016;36:5055–70.
 44. Gao YJ, Ji RR. Targeting astrocyte signaling for chronic pain. *Neurotherapeutics* 2010;7:482–93.
 45. Ji RR, Berta T, Nedergaard M. Glia and pain: is chronic pain a gliopathy? *Pain* 2013;154 Suppl 1:S10–28.
 46. Cui YH, Le Y, Gong W, Proost P, van Damme J, Murphy WJ, et al. Bacterial lipopolysaccharide selectively up-regulates the function of the chemotactic peptide receptor formyl peptide receptor 2 in murine microglial cells. *J Immunol* 2002;168:434–42.
 47. Kong Y, Ruan L, Qian L, Liu X, Le Y. Norepinephrine promotes microglia to uptake and degrade amyloid β peptide through upregulation of mouse formyl peptide receptor 2 and induction of insulin-degrading enzyme. *J Neurosci* 2010;30:11848–57.
 48. Lee Y, Pai M, Brederson JD, Wilcox D, Hsieh G, Jarvis MF, et al. Monosodium iodoacetate-induced joint pain is associated with increased phosphorylation of mitogen activated protein kinases in the rat spinal cord. *Mol Pain* 2011;7:39.
 49. Macdonald LJ, Boddy SC, Denison FC, Sales KJ, Jabbour HN. A role for lipoxin A₄ as an anti-inflammatory mediator in the human endometrium. *Reproduction* 2011;142:345–52.